Malaysian Journal of Chemistry, 2023, Vol. 25(3), 303-313
(Special Issue: *3rd IKMPB Online Symposium 2023 - Innovation in Chemistry Towards Sustainable Development*)

Structural, Morphological and Magnetic Property Evolution of Dye-Loaded Magnetic Bentonite Composite for Reusability Studies

Nur Syafiqah Alisa Mohd Nizam[1], Siti Nor Atika Baharin[1], Binoy Sarkar[2] and Ruhaida Rusmin[1]*
[1]Faculty of Applied Sciences, Universiti Teknologi MARA, Cawangan Negeri Sembilan, Kampus Kuala Pilah 72000 Kuala Pilah, Negeri Sembilan, Malaysia
[2]Future Industries Institute, University of South Australia, Mawson Lakes, SA 5095, Australia
*Corresponding author (e-mail: ruhaida@uitm.edu.my)

Reusability of adsorbent has gained significant research interest in the pursuit of sustainable environmental protection. This study aims to investigate the structural and morphological evolution of a dye-loaded magnetic bentonite composite (MBC) and its reusability for dye removal from water over multiple adsorption-desorption cycles. The magnetic susceptibility, structural and morphological properties of the spent magnetic bentonite composite (SMBC) were characterized by using vibrating sample magnetometer (VSM), Fourier transform infrared (FTIR) spectroscopy, x-ray powder diffraction (XRD), scanning electron microscopy coupled with energy dispersive x-ray (SEM-EDX) spectrometry and transmission electron microscopy (TEM). Desorption eluents (NaCl, NaOH, HCl, ethanol and deionized water) were used to investigate the dye desorption efficiency from SMBC. The magnetic susceptibility and morphological properties of the regenerated SMBC were also determined. FTIR results and EDX analysis confirmed the adhesion of methylene blue (MB) dye on MBC. The dye-loaded MBC retained its magnetization strength (11.9 emu/g); however, TEM and SEM images showed increasingly loose morphologies. The 0.1 M NaCl eluent recorded the highest desorption efficiency (64%) following three adsorption-desorption cycles. The magnetic strength and adsorption efficiency of the reused MBC (RMBC) were reduced after the third cycle. The desorption experiment could be further optimized for enhanced reusability of SMBC. Harsh conditions (e.g., higher concentration of eluent) may affect the stability of the regenerated adsorbent, thus warranting future research.

Keywords: Magnetic clay composite; adsorption-desorption; reusability; adsorbent stability

Received: December 2022; Accepted: April 2023

Textile and garment manufacturing industries are considered as Malaysia's important economic sector that contributes significantly toward the country's wealth and economic growth. Nevertheless, one of the major environmental sustainability challenges faced by these industries lies in the improper management of effluents containing numerous organic and inorganic pollutants including dyes and heavy metals. For instance, effluent from the batik industries often contains azo, triarylmethane, and anthraquinone dyes [1]. Methylene Blue dye, MB, (chemical formula of $C_{16}H_{18}N_3SCl$) (Figure 1a) is an example of azo dye usually used in the textile and pharmaceutical industries and is known to be hazardous to aquatic life if not properly treated. In wastewater treatment, adsorption technique is a favorable approach in treating dye contaminated water because of its straightforward process and high efficiencies as compared to flocculation and electro-chemical methods [2]. Clay minerals, a group of natural aluminosilicates, are often selected as the adsorbent for removing water pollutants due to their natural abundancy, low toxicity, and high capabilities in adsorbing water contaminants such as dyes. For example, bentonite clay (chemical formula of $Al_2H_2Na_2O_{13}Si_4$) (Figure 1b) has been previously used in water treatment of dyes with an excellent performance [3,4,5].

Hybrid materials like magnetic clay composite are currently receiving a great demand in water treatment applications because of their versatile surface properties and simple preparation method. Several types of magnetic clay such as kaolinite-iron oxide [6,7], and magnetic sepiolite [8] have been developed with promising results in removing water pollutants. More importantly, with the presence of iron oxide embedded in the clay composite, these magnetic clays offer easy magnetic separation of the spent adsorbents via external magnetic field. This modification helps to address the current recovery issue of spent clay adsorbents that require conventional filtration or centrifugation which are tedious, costly and energy consuming.

†Paper presented at the 3rd IKMPB Online Symposium 2023 - Innovation in Chemistry Towards Sustainable Development

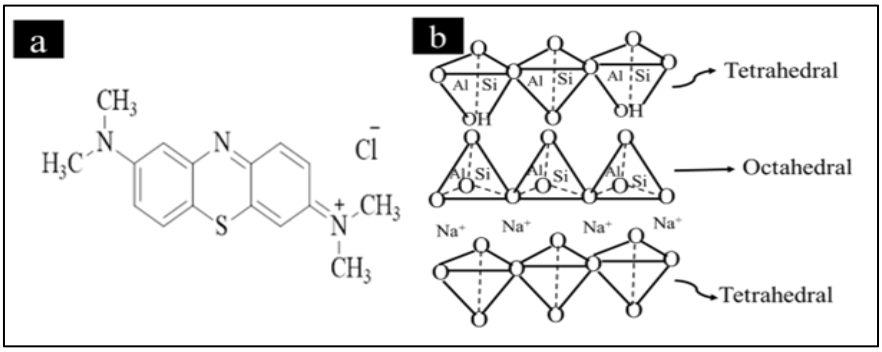

Figure 1. Structure of (a) MB and (b) bentonite.

The adsorbent that has been retrieved from the treatment media is known as a spent adsorbent. In order to make the wastewater treatment process feasible, sustainable, and economical, it is important to recycle the spent adsorbent [1]. Spent adsorbents are usually disposed of through incineration or landfilling which could pose a secondary pollution problem if leaching occurs. Hence, recycling of spent adsorbents is the preferred approach to reduce the overall cost of treatment, alleviate disposal problems, and reduce sludge production. The success in recycling depends on the several factors; like the feasibility of contaminant desorption (or adsorbent recoveries), and capability of the spent adsorbent to maintain its structural integrities while sustaining its efficiencies in numerous adsorption-desorption cycles before the adsorbent become exhausted. Within this direction, most research only reports about the desorption percentage and numbers of consecutive cycles successfully achieved for a spent adsorbent [1,9,10,11,12]. However, very little focus was given toward the assessment of structural and morphological changes of spent adsorbents to correctly evaluate their suitability in sustaining the recycling process. Discussion on the surface characteristics of the regenerated adsorbent is scarce; thus, further understanding on the transformation, mobility, and fate of the adsorbent toward sustainable waste management is needed.

This study aims to assess the changes in structural, morphological, and magnetic properties of magnetic bentonite composite (MBC) upon interaction with MB dye as a model pollutant. To favor the adsorption of MB molecules, it is hypothesized that some changes in the surface porosity, texture, and active sites of MBC would occur leading to textural changes and reduction of magnetic properties of the composite to some extent. Such changes are expected to be more evident during adsorption-desorption cycles in reusability studies. To validate this hypothesis, spectroscopic and macroscopic techniques were applied together with magnetic measurements of the spent magnetic bentonite composite (SMBC). The characterization results were used to deduce the stability of the composite for forecasting any potential functionality or structure deterioration (e.g., loss of magnetic properties or porosity). The SMBC was subjected to desorption-adsorption cycles and the structural transformation of reused MBC (RMBC) was observed.

EXPERIMENTAL

Chemicals and Materials

Raw bentonite clay (Sigma-Aldrich) supplied by MC Lab Supplies Sdn. Bhd. (Malaysia) was sieved (200 mesh) and used directly without purification. Methylene blue (minimum 82% purity) and ammonium hydroxide (NH_4OH, 25%) were supplied by Systerm® (Malaysia). The iron(III) chloride hexahydrate ($FeCl_3.6H_2O$, 98%) was supplied by HmbG® Chemicals (Germany) while iron(II) sulphate heptahydrate ($FeSO_4.7H_2O$, 99.9% assay), sodium chloride (NaCl, 99.8% assay) were supplied by Bendosen (Malaysia). Ethanol (C_2H_5OH, 95% assay), was obtained from Systerm® (Malaysia).

Preparation of Fresh and Spent Magnetic Bentonite Composite

The magnetic bentonite composite (MBC) was freshly prepared via co-precipitation technique in a one-pot synthesis route [6]. $FeCl_3.6H_2O$ of 3.1 g and $FeSO_4.7H_2O$ of 2.4 g were separately dissolved in 50 mL of deionized water. The Fe^{3+} solution was then mixed with 4 g of raw bentonite and the mixture was placed in an ultrasonic bath at 40°C for 15 min. Next, the mixture was transferred to a water bath (Wise Bath, WSB-30 WITEG) and the Fe^{2+} solution prepared earlier was then added to the Fe^{3+}- bentonite mixture. The Fe^{2+}- Fe^{3+}-bentonite suspension was agitated (200 rpm) at 60°C for 30 min. Dropwise of NH_4OH (25 %v/v) was slowly added to the suspension for 60 min (to achieve pH 9) with a rapid agitation (400 rpm) to yield a brownish-black precipitate. The suspension was left to react for another 120 min under N_2 atmosphere before being filtered. The precipitate MBC was washed thoroughly with deionized water and ethanol until the supernatant reached pH 7. The MBC was dried at 110°C for 4 h, ground and sieved (200 mesh), and kept in a sealed dark container for further use.

The prepared MBC was used to remove MB dye through batch adsorption experiments. The experiments were carried out at initial MB concentration of 50 mg/L under optimized conditions retrieved from preliminary works (adsorbent loading = 1.0 g/L, agitation speed = 130 rpm, temperature = 25°C, contact time = 1 h, pH of solution = 6). Then, the spent magnetic bentonite composite (known as SMBC) was recovered from the suspension by placing an external magnetic field using a magnetic bar. The dye concentration was determined by using the UV-Vis spectrophotometer (T80+, PG Instrument Ltd.) in duplicates, at a maximum MB wavelength of 663 nm. The adsorption capacity, q_e and the removal efficiency (%) towards MB dye was calculated by using Equation 1 and Equation 2 respectively:

$$q_e = \frac{(C_o - C_e)\ m}{V} \quad (1)$$

$$\text{Removal efficiency (\%)} = \left[\frac{C_o - C_e}{C_o}\right] \times 100 \quad (2)$$

Where q_e (mg/g) is adsorption capacity, C_o is initial concentration of MB (mg/L), C_e (mg/L) is equilibrium concentration of MB, V is volume (L) of the MB solution and m is mass (g) of the composite.

Adsorption-desorption and Reusability Study

The SMBC retrieved from the adsorption experiment was immersed in various desorption eluents (deionized water, ethanol-water (70:30) mixtures and 0.1 M of NaCl, NaOH, and HCl, respectively). The SMBC was agitated (130 rpm) in a 100 mL aqueous solution of each desorbing eluent for 1 h. Agitation is needed to ensure a homogenous dispersion of SMBC in the desorption eluent. The amount of desorbed MB in suspension from SMBC was determined by using the UV-Vis spectrometer. The desorption percentage was calculated according to Equation 3.

$$\text{Desorption efficiency (\%)} = \frac{\text{concentration of dye desorbed by eluent}}{\text{concentration of dye adsorbed on adsorbent}} \times 100 \quad (3)$$

Meanwhile, for reusability studies, the SMBC collected after the desorption using 0.1 M of NaCl was used. After desorption, the composite was washed thoroughly with distilled water and underwent the adsorption-desorption process as described earlier, up to three cycles. The reused MBC (assigned as RMBC) from the reusability study was collected, dried at 60°C for 4 h and ground for further characterization studies.

Characterization of Magnetic Bentonite Composite Pre- and Post- Adsorption

FTIR spectrum of MBC, SMBC and RMBC were acquired by using Fourier-transform infrared (FTIR) spectrometer (Perkin Elmer Spectrum 100) with a resolution of 4 cm^{-1} in the range of 4000 cm^{-1} – 600 cm^{-1} with 16 scans. Magnetic property measurements of MBC, SMBC and RMBC were carried out using Lake Shore 340 VSM at 25°C, with an applied magnetic field up to 8000 Oe with 200 points plots. The speed of MBC in the aqueous solution to respond and attract towards the external magnetic bar (Neodymium) placed outside the reaction container was measured (in seconds) using a digital stopwatch. XRD data of MBC and SMBC were collected by X'Pert[3] Powder X-ray diffractometer using Cu-Kα radiation with a setting voltage at 40 kV and 40 mA current. The XRD pattern was acquired from a 2θ range between 5° to 80° with a step size of 0.03°. Scanning electron microscopy (SEM) images of MBC and SMBC were captured on an FEI Quanta 200 SEM at 15kV to observe the morphology and estimate the particle size of the samples. The samples were prepared by direct deposition on an aluminum stub covered by a carbon grid and then coated with a thin layer of gold (~10 nm thick film). The energy dispersive x-ray (EDX) analysis of MBC and SMBC were performed simultaneously to determine the elemental composition (Al, Si, O, Fe, etc.). Lastly, transmission electron microscopy (TEM) analysis of MBC and SMBC were carried out using the TEM Talos L120C model at 120 kV acceleration voltage to determine the particle size and morphologies of the samples at nanoscale.

RESULTS AND DISCUSSION

Characterization of the Fresh and Spent Magnetic Bentonite Composite

FTIR Analysis

Figure 2a shows the FTIR spectra of MBC and spent magnetic bentonite composite (SMBC). For MBC, a fingerprint band of bentonite occurred at 3626 cm^{-1} corresponding to the (Si,Al)-OH stretching vibration on the silicate surface of these clays [10] while an inter-layer water band in bentonite appeared at 3329 cm^{-1}. These functional groups are often considered as binding sites for cationic species like MB dye towards bentonite-based materials [10]. The band at 1629 cm^{-1} was attributed to the bending HO-H bond of water molecules retained in the silicate matrix [11]. Meanwhile, the spectral band at 1448 cm^{-1} in MBC was probably due to the NH_2 bending originating from the ammonium hydroxide used during the synthesis [13]. A sharp band at 879 cm^{-1} in MBC indicated a successful inclusion of iron oxide in the clay as it represented the formation of Al-Fe-OH interaction [14].

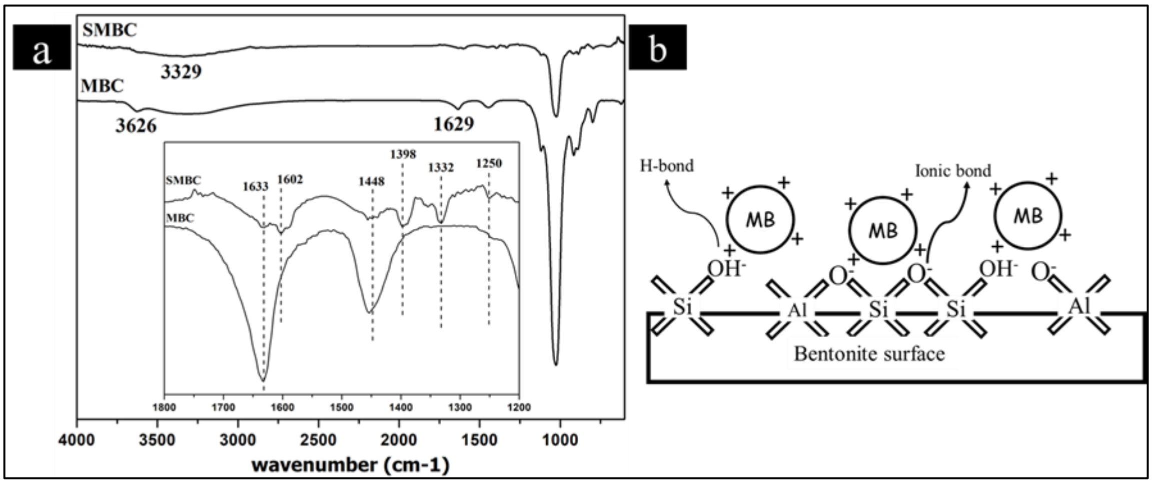

Figure 2. FTIR spectra of (a) MBC and SMBC and (b) schematic diagram to illustrate MB-MBC interaction occurred during the adsorption process.

In SMBC, the band intensity for OH stretching at 3626 cm^{-1} (assigned to (Si,Al)-OH)) and 3329 cm^{-1} (interlayer water band in bentonite) previously seen in MBC has weakened (Figure 2a). This observation suggested the interaction on the aluminosilicate surface with the MB occurs via electrostatic interaction (e.g., ionic bond and hydrogen bonds) as illustrated in Figure 2b. Furthermore, the intense bands corresponding to the symmetric and asymmetric C-H stretching vibration of $-CH_3$ exist in the structure of MB can be seen at 1398 cm^{-1} and 1332 cm^{-1}. In addition, the band belonging to the water molecule at 1633 cm^{-1} has weakened in the silicate layer in SMBC due to hydrogen bonding with N^+ in MB during the adsorption process [1]. The bands at 1602 cm^{-1} and 1448 cm^{-1} were due to the C=C stretching vibration from the aromatic rings of methylene blue. Besides, the band at 1250 cm^{-1} in SMBC indicated CN- stretching which further confirmed the existence of MB on the composite. Meanwhile, the vibration band near 1116 cm^{-1} assigned to the hydroxyl group of Fe-OH became less intense probably due to the accumulation of MB on the surface of SMBC [15].

VSM Analysis

The saturation magnetization value, M_s of MBC is 10.6 emu/g (Table 1), which is higher than the previously reported value for other magnetic clay [2,16]. The VSM plot produced a very small hysteresis loop with the “S”-shape curve passing through the zero point of magnetization (Figure 3). These features were associated with a near superparamagnetic characteristic material [10]. Previous findings indicated that magnetic adsorbent may lose its magnetic susceptibility upon interaction with contaminants, due to the presence of nonmagnetic materials in the synthesized composite particles [6]. For example, after the adsorption of phosphate using porous magnetic biochar (PMB), the magnetic strength was greatly decreased to 28.4 emu/g from the initial value of 38.9 emu/g [17].

On the contrary, this study’s findings showed that SMBC had a slight increase in M_s, retentivity (M_r) and coercivity (H_c) values (Table 1). These findings could be associated with the changes in morphology, particle size and concentration of iron oxide clusters within the composite [18, 19] due to surface coverage with bulky MB in SMBC. Nevertheless, with the presence of MB dye-loaded into the composite, the material still showed a fast response towards the external magnetic field (accumulation achieved within 69±2 s, on average).

Table 1. Magnetism properties of MBC, SMBC and RMBC.

Sample	Magnetization, M_s (emu/g)	Coercivity, H_c (G)	Retentivity, M_r (emu/g)
MBC	10.6	33.5	0.82
SMBC	11.9	40.4	1.03
RMBC	5.5	35.5	0.58

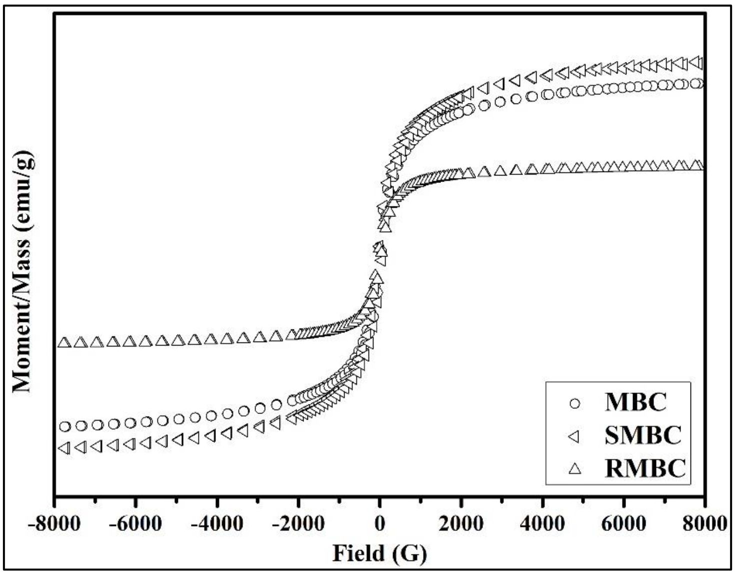

Figure 3. VSM curves of MBC, SMBC and RMBC.

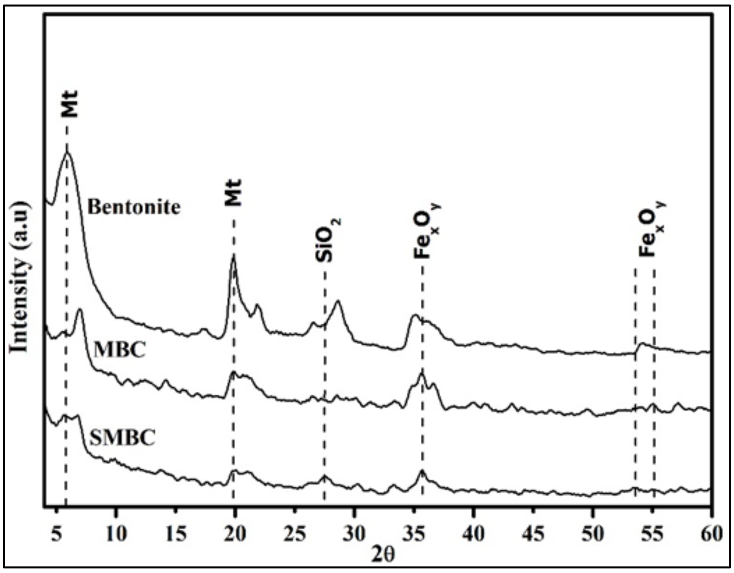

Figure 4. XRD pattern for Bentonite, MBC and SMBC. Mt: montmorillonite, SiO_2: quartz, Fe_xO_y: iron oxide.

XRD Analysis

Bentonite consists mainly of quartz (SiO_2, 2θ = 26.6°) and montmorillonite (Mt, 2θ = 5.9°, 20°) phase, with some impurities like calcite and feldspar [15]. In MBC, the diffraction peak representing bentonite (2θ = 7° and 20°) was intense (Figure 4). New peaks assigned to the Fe_xO_y (2θ = 35.7°, 54.9° and 57.0°) were also present which indicated the successful adhesion of iron oxide particles on the surface of the bentonite [20]. Meanwhile in SMBC, all major peaks observed in MBC were retained which portrayed the structural stability of the composite. The intensity of montmorillonite peaks at 2θ = 7° and 20° was decreased significantly due to the adhesion of dye molecules. This is in accordance with the interaction of the dye molecule with the functional groups of bentonites serving as main active sites as postulated in FTIR analysis described previously. The peak intensity of iron oxide, particularly at 2θ = 35.7° and 54.9° was slightly reduced in SMBC which suggested partial involvement of this substance in MB adsorption toward MBC.

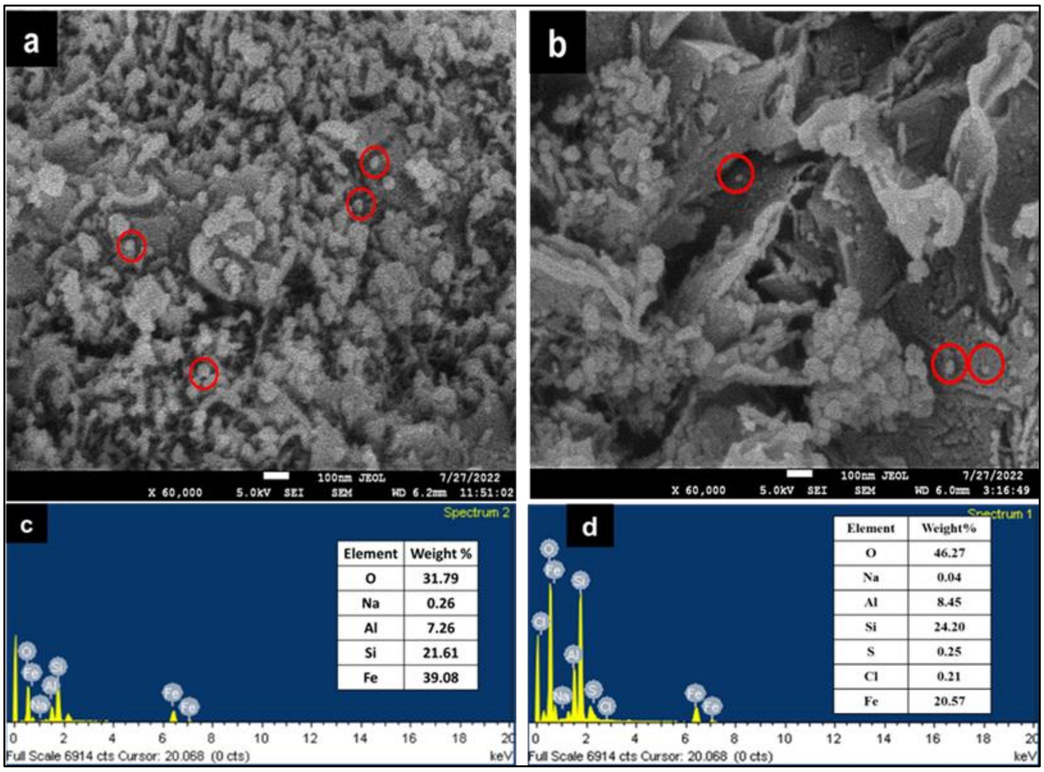

Figure 5. SEM images of (a) MBC and (b) SMBC, with iron oxide in circle with EDX spectra comparison between (c) MBC and (d) SMBC.

SEM-EDX Analysis

The SEM image of MBC showed the aggregation of iron oxide particles observed on the surface of bentonite. The bentonite layers typically have a rough surface and are closely stacked together [20,21] but in MBC (Figure 5a), smaller segments were generated that produce more porosity [22]. Meanwhile in SMBC, the surface roughness had decreased leaving behind cleaner surface. The bentonite layers become less dense but remain intact (Figure 5b). In addition, iron oxide clusters were dispersed more on bentonite surface in SMBC as compared to those observed in MBC. The exposed and loose iron oxide aggregates as observed in this SEM image could possibly contribute to a higher magnetization saturation as described earlier in VSM analysis, due to suppress of interparticle magnetic interaction. EDX analysis of both composites confirmed the presence of Fe coming from iron oxide (Figure 5c) with less percentage (20.57%) was observed in SMBC (Figure 5d). In addition, the presence of elemental chlorine (Cl) and sulfur (S) in SMBC was originated from the adsorbed MB molecule.

TEM Analysis

Figure 6 shows the TEM image of MBC, SMBC and the size of iron oxide embedded in the composite. A distribution of spherical, flakes and rod-like particles associated with iron oxide were present in both MBC (Figure 6a) and SMBC (Figure 6c). Iron oxide nanoparticles (magnetite or maghemite) commonly existed in spherical shapes, but anisometric iron oxide particles with different morphology like flower, nanorods and cubes were recently gaining significant research interests [23, 24]. On average, the diameter of each iron oxide particle in MBC was 9 nm while the length ranges from 29 nm to 32 nm (Figure 6b). The reported size of iron oxide obtained was within the diameter range in previous study [25, 26]. It also can be seen clearly that the iron particles were tightly bound and uniformly dispersed on top of the bentonite surface. The presence of this heterostructure was attributed to the strong bonds between Si-O, Al-O, O-H, Si-O-Si and Si-O-Al of bentonite with the Fe-O contained in iron oxide [27].

Meanwhile, the TEM image of SMBC (Figure 6c) clearly showed more expanded layers of bentonite which parallel with the observation obtained on its SEM image previously described (Figure 5b). The accumulation of iron oxide particles was less dense, and the clusters scattered throughout the bentonite surface, implying morphological changes faced by SMBC to accommodate the MB dye molecules. The size of the iron oxide particles in SMBC (Figure 6d) was increased between from 50 nm to 57 nm as compared to previous length recorded in MBC (29 to 32 nm) (Figure 6b). The increment in the particle size hence explains the increase in M_s value [19] of SMBC as compared to the MBC as described earlier during the VSM analysis.

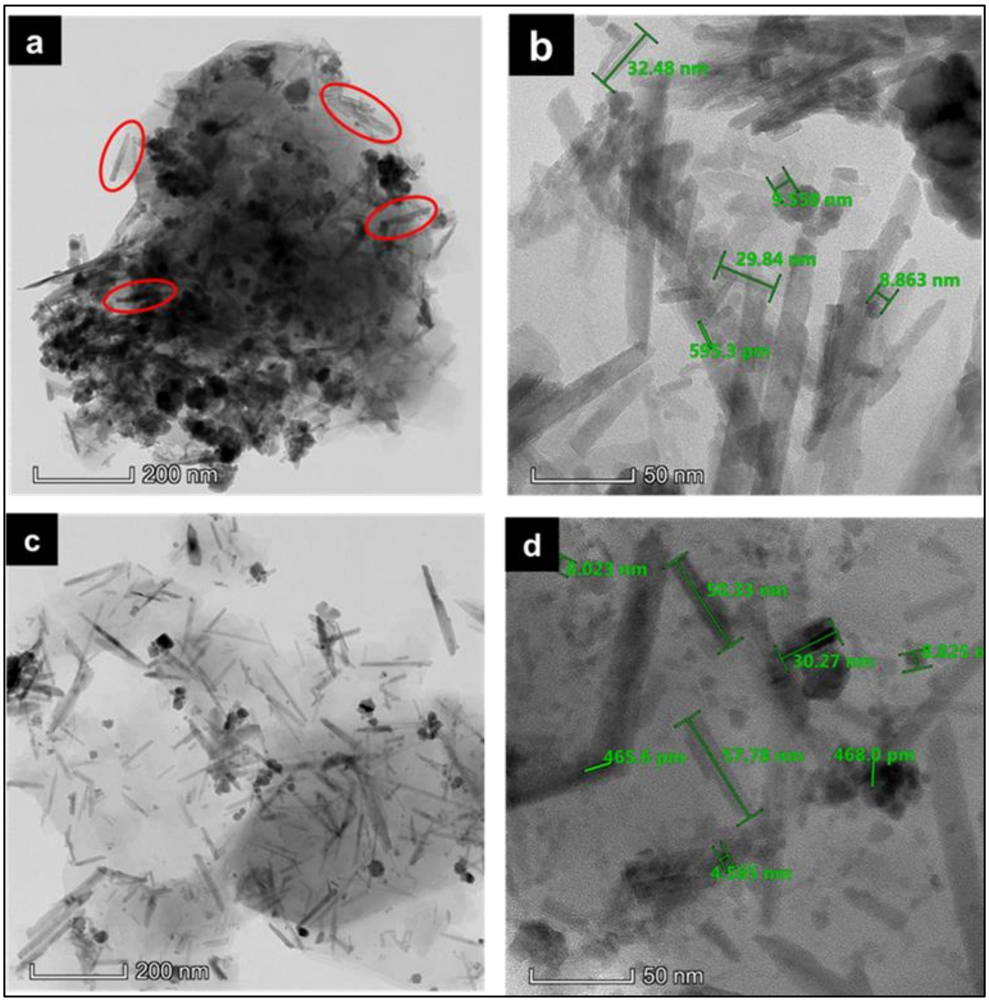

Figure 6. TEM images of (a) MBC with iron oxide in circle, (b) the size of the iron oxide in MBC and (c) SMBC and (d) the size of iron oxide in SMBC.

Adsorption-desorption Study

The desorption of pollutants from spent adsorbent is an important factor to ensure successful reusability of the adsorbent. If a high desorption occurs when using water as the eluent, the pollutant-adsorbent interaction is more likely a physisorption. Whereas the desorption using strong eluents like acids or salt suggest involvements of chemisorption interaction [28]. In this study, the adsorption capacity of MBC recorded from the batch adsorption study was 49.8 mg/g with a 100% MB removal efficiency. This complete removal of MB indicates that all MB in the aqueous solution has been successfully loaded into the MBC. The desorption of the embedded MB in the MBC using a 0.1 M NaCl with suitable agitation yielded the highest MB desorption, 64.8%, as compared to other eluents (Figure 7). Direct observation of the color of desorption solution also indicated the successfulness of MB desorption (Figure 7, inset). Ion exchange reactions and the suppression of surface charge in SMBC in high ionic strength as in NaCl may result in a higher MB released from the MBC [29,30]. This is ascribed to the cation exchange mechanism occurring between Na^+ with the loaded-MB^+ is greater, contributed to a high MB in the solution. On a different perspective, high retention of MB in SMBC even against acidic and base eluents indicates the strong MB-SMBC interaction that prevents leaching of the adsorbed MB molecules thus low desorption. While those acid/base eluents are commonly used, NaCl is considered as a more cost-effective and environmentally friendly desorption agent [30]. Hence, from the point of environmental perspective, desorption using NaCl is much favorable.

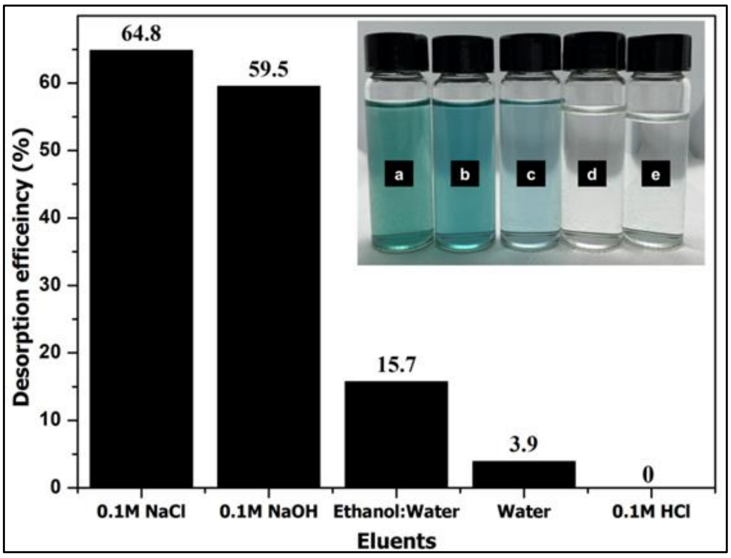

Figure 7. Desorption percentage of MB from SMBC using various eluents. (Inset picture: colour of eluent retrieved from desorption study, where a = NaCl; b = NaOH; c= 70:30 ethanol: water solution; d= deionized water; and e= HCl).

Recycling and the Stability of the Reused Magnetic Bentonite Composite (RMBC)

Recycling of an adsorbent is an important parameter from the economic and environmental perspective when operating water treatment process. An ideal adsorbent should retain its efficiencies even after multiple cycles. As shown in Figure 8, the removal efficiency of RMBC remained high at the second cycle which implied the high stability and performance of MBC. However, the removal efficiency significantly dropped to 50% after the third cycle following the low desorption percentage (8%) on the second cycle. While NaCl may trigger the MB released from SMBC, the salinity also may progressively change the surface activity and aggregation of MB. It was reported that high ionic strength may cause aggregation of particles on the surface. Therefore, the adsorbed molecules were more tightly adhered to the adsorbent causing irreversible dye adsorption on the solid surface [31]. The inability of adsorbed MB to be removed from the active sites during the desorption experiment led to a reduction in the number of active sites available for subsequent cycles. To investigate the cause of declining MB adsorption efficiencies, spectroscopic investigation using FTIR and measurement of magnetic strength of RMBC was carried out.

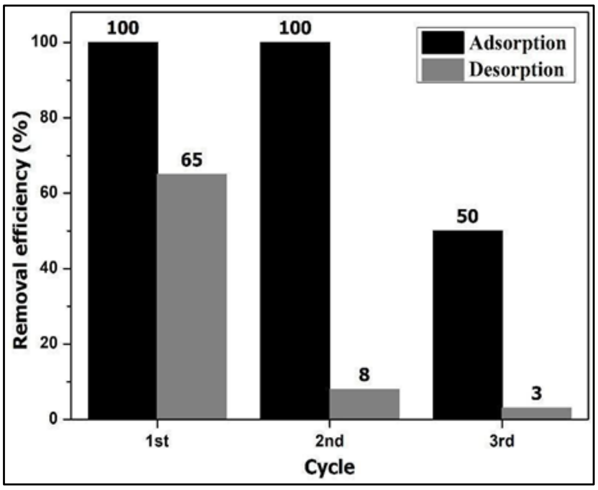

Figure 8. Adsorption-desorption cycle of MBC using 0.1 M NaCl as desorption eluent.

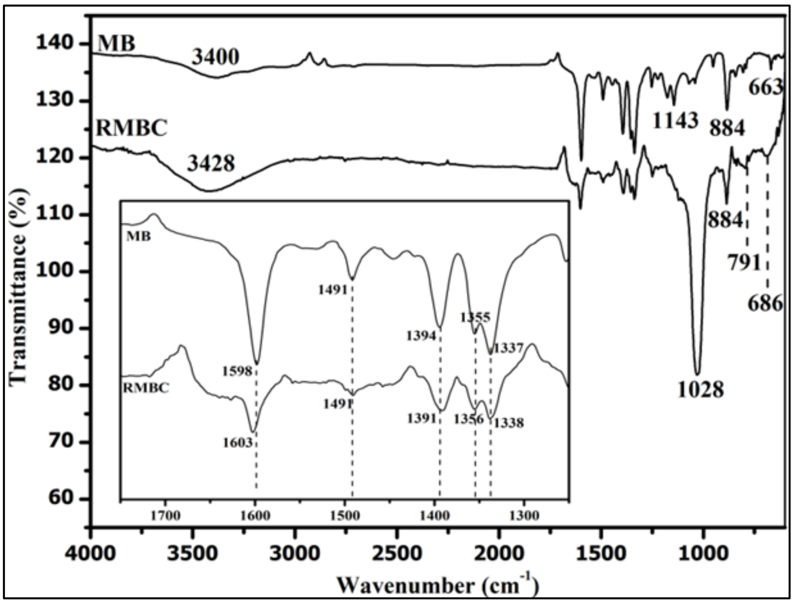

Figure 9. FTIR spectra of MB and RMBC.

Figure 9 shows the FTIR spectra of MB and RMBC. All the MB bands previously seen in SMBC (Figure 2) were present in the RMBC spectrum, for example the skeletal vibration of aromatic and stretching of C-N of MB at 884 cm^{-1} [32]. The intensity of bands associated with MB were increased in RMBC, implying more MB was adhered towards RMBC after the third cycle. Hence, it confirmed the accumulation of MB after three cycles which caused lower desorption aforementioned. In addition, the iron oxide bands at 686 cm^{-1} (Al-Fe-OH bands) in the RMBC remained intact indicating the perseverance of this particles even after three cycles [14].

While FTIR shows the existence of iron oxide remaining in RMBC, the VSM analysis findings reveal the decrease in magnetic strength as compared to MBC and SMBC (Table 1). It is postulated that the M_s decline is due to progressive adsorption-desorption cycle faced by RMBC, in addition to the large presence of nonmagnetic MB particles adhered to the surface. Therefore, more assessment of the structural integrity needs to be carried out to ensure the practicality and stability of magnetic clays to sustain multiple reusability cycles.

CONCLUSION

In this study, MBC was successfully prepared and characterized pre- and post-adsorption experiments with MB dye. The functional groups and magnetic properties of MBC and SMBC were preserved. However, significant changes in the morphological properties were observed via SEM and TEM analyses. MB desorption of 64% from SMBC was achieved using 0.1 M NaCl as the desorbing eluent after three successful adsorption-desorption cycles. The dye removal efficiency was reduced to 50% in the final cycle, denoting a possible structural deterioration and saturation of active sites of the exhausted adsorbent. These changes were accompanied by a decline in magnetic strength (as observed in RMBC) possibly due to the accumulation of MB and leaching or passivation of iron oxides. Future works need to focus on optimizing the recycling conditions (i.e., choice of eluent and contact hour for desorption) to ensure a more successful reusability of MBC. Advanced atomic scale characterization techniques are needed for comprehensive assessment of the structural stability of magnetic clay composite particularly when applied for water treatment at industrial scale. The findings of this study are expected to give a fresh insight on the environmental transformation of engineered materials such as magnetic clay for advanced and sustainable waste-water remediation.

ACKNOWLEDGEMENTS

The authors would like to thank Universiti Teknologi MARA through the Young Talent Researcher (YTR) grant (File No.: 600-RMC/YTR/5/3 (006/2020)) for the financial support to conduct this research. Partial funding through the Fundamental Research Grant Scheme (FRGS) (Grant No.: FRGS/1/2019/STG07/UITM/02/15) supported by the Ministry of Higher Education, Malaysia is greatly acknowledged. The authors are grateful to the Nanotechnology & Catalysis Research Centre (NANOCAT), University of Malaya, Malaysia for technical assistance in VSM measurement. Assistance in preliminary laboratory works from Izzan Salwana Izman (Universiti Teknologi MARA, Negeri Sembilan) and unanimous technical advice from the project members are appreciated. The authors declare that they have no conflict of interest.

REFERENCES

1. Momina, Mohammad, S. & Suzylawati, I. (2020) Study of the adsorption/desorption of MB dye solution using bentonite adsorbent coating. *Journal of Water Process Engineering*, **34**, 101155.

2. Ain, Q. U., Rasheed, U., Yaseen, M., Zhang, H. & Tong, Z. (2020) Superior dye degradation and adsorption capability of polydopamine modified Fe_3O_4-pillared bentonite composite. *Journal of Hazardous Materials*, **397**, 122758.

3. Alexander, J. A., Ahmad Zaini, M. A., Surajudeen, A., Aliyu, E. N. U. & Omeiza, A. U. (2019) Surface modification of low-cost bentonite adsorbents: A review. *Particulate Science and Technology*, **37(5)**, 534–545.

4. Santos, S. S. G., França, D. B., Castellano, L. R. C., Trigueiro, P., Silva Filho, E. C., Santos, I. M. G. & Fonseca, M. G. (2020) Novel modified bentonites applied to the removal of an anionic azo dye from aqueous solution. *Colloids and Surfaces: Physicochemical and Engineering Aspects*, **585**, 124152.

5. Taher, T., Rohendi, D., Mohadi, R. & Lesbani, A. (2019) Congo red dye removal from aqueous solution by acid-activated bentonite from sarolangun: Kinetic, equilibrium, and thermodynamic studies. *Arab Journal of Basic and Applied Sciences*, **26(1)**, 125–136.

6. Izman, I. S., Johan, M. R. & Rusmin, R. (2022) Insight into Structural Features of Magnetic Kaolinite Nanocomposite and Its Potential for Methylene Blue Dye Removal from Aqueous Solution. *Bulletin of Chemical Reaction Engineering & Catalysis*, **17(1)**, 205–215.

7. Salleh, N. F. A., Izman, I. S., Johan, M. R. & Rusmin, R. (2021) Influence of pH on the structural and magnetism stability of magnetic kaolinite composite. *AIP Conference Proceedings*, **2368(6)**, 020001.

8. Xu, X., Chen, W., Zong, S., Ren, X. & Liu, D. (2019) Magnetic clay as catalyst applied to organics degradation in a combined adsorption and Fenton-like process. *Chemical Engineering. Journal*, **373(2)**, 140–149.

9. Azha, S. F., Sellaoui, L., Engku Yunus, E. H., Yee, C. J., Bonilla-Petriciolet, A., Ben Lamine, A. & Ismail, S. (2019) Iron-modified composite adsorbent coating for azo dye removal and its regeneration by photo-Fenton process: Synthesis, characterization, and adsorption mechanism interpretation. *Chemical Engineering Journal*, **361**, 31–40.

10. Jiang, L., Ye, Q., Chen, J., Chen, Z. & Gu, Y. (2018) Preparation of magnetically recoverable bentonite–Fe_3O_4–MnO_2 composite particles for Cd(II) removal from aqueous solutions. *Journal of Colloid and Interface Science*, **513**, 748–759.

11. Eltaweil, A. S., Mohamed, H. A. & El-Monaem, E. M. A. (2020) Mesoporous magnetic biochar composite for enhanced adsorption of malachite green dye: Characterization, adsorption kinetics, thermodynamics, and isotherms. *Advanced Powder Technology*, **31**, 1253–1263.

12. Jiang, M., Niu, N. & Chen, L. (2022) A template synthesized strategy on bentonite-doped lignin hydrogel spheres for organic dyes removal. *Separation and Purification Technology*, **285**, 120376.

13. Tahir, H. B., Abdullah, R. M. & Aziz, S. B. (2022) The H^+ ion transport study in polymer blends incorporated with ammonium nitrate: XRD, FTIR, and Electrical characteristics. *Results in Physics*, **42**, 105960.

14. Sanad, M. M. S., Farahat, M. M. & Abdel Khalek, M. A. (2021) One-step processing of low-cost and superb natural magnetic adsorbent: kinetics and thermodynamics investigation for dye removal from textile wastewater. *Advanced Powder Technology*, **32(5)**, 1573–1583.

15. Wang, B., Zhang, H., Hu, X., Chen, R., Guo, W., Wang, H., Wang, C., Yuan, J., Chen, L. & Xia, S. (2022) Efficient phosphate elimination from aqueous media by La/Fe bimetallic modified bentonite: Adsorption behavior and inner mechanism. *Chemosphere*, **312**, 137149.

16. Esvandi, Z., Foroutan, R., Jamaleddin, S., Akbari, A. & Ramavandi, B. (2020) Uptake of anionic and cationic dyes from water using natural clay and clay/starch/Mn-Fe_2O_4 magnetic nanocomposite. *Surfaces and Interfaces*, **21**, 100754.

17. Tomin, O. & Yazdani, M. R. (2022) Production and characterization of porous magnetic biochar: Before and After Phosphate Adsorption Insights. *Journal of Porous Materials*, **29(3)**, 849–859.

18. Shafiee, M., Foroutan, R., Fouladi, K., Ahmadlouydarab, M. & Ramavandi, B. (2018) Application of oak powder/Fe_3O_4 magnetic composite in toxic metals removal from aqueous solutions. *Advanced Powder Technology*, **12**, 2172.

19. Yamaura, M. & Alves, D. (2013) Synthesis and characterization of magnetic adsorbent prepared by magnetite nanoparticles and zeolite from coal fly ash. *Journal Material Science*, **48**, 5093–5101.

20. Lou, Z., Zhou, Z., Zhang, W., Zhang, X., Hu, X., Liu, P. & Zhang, H. (2015) Magnetized bentonite by Fe_3O_4 nanoparticles treated as adsorbent for methylene blue removal from aqueous solution: Synthesis, characterization, mechanism, kinetics, and regeneration. *Journal of the Taiwan Institute of Chemical Engineering*, **49**, 199–205.

21. Ghohestani, E., Samari, F. & Yousefinejad, S. (2022) An efficient removal of methylene blue and lead(II) from aqueous solutions by green synthesized iron oxide/pillared bentonite nano-composite. *Materials Chemistry and Physics*, **287**, 126266.

22. Shabani, E., Salimi, F. & Jahangiri, A. (2018) Removal of Arsenic and Copper from Water Solution Using Magnetic Iron/Bentonite Nano-particles (Fe_3O_4/Bentonite). *Silicon*, **11**, 961-971.

23. Roca, A. G., Gutiérrez, L., Gavilán, H., Brollo, E. F., Veintemillas-verdaguer, S. & Morales, M. del P. (2019) Design Strategies for Shape-Controlled Magnetic Iron Oxide Nanoparticles. *Advanced Drug Delivery Reviews*, **138**, 68–104.

24. Jassal, V. & Gahlot, S. (2016) Green synthesis of some iron oxide nanoparticles and their interaction with 2-Amino, 3-Amino and 4-Aminopyridines. *Materials Today: Proceedings*, **3(6)**, 1874–1882.

25. Abdullah, N. H., Shameli, K., Abdullah, E. C. & Abdullah, L. C. (2020) Low cost and efficient synthesis of magnetic iron oxide/activated sericite nanocomposites for rapid removal of methylene blue and crystal violet dyes. *Materials Characterization*, **163**, 110275.

26. De Marco, C., Mauler, R. S., Daitx, T. S., Krindges, I., Cemin, A., Bonetto, L. R., Crespo, J. S., Guégan, R., Carli, L. N. & Giovanela, M. (2020) Removal of malachite green dye from aqueous solutions by a magnetic adsorbent. *Separation Science and Technology (Philadelphia)*, **55(6)**, 1089–1101.

27. Barakan, S. & Aghazadeh, V. (2019) Synthesis and characterization of hierarchical porous clay heterostructure from Al-Fe-pillared nano-bentonite using microwave and ultrasonic techniques. *Micro-porous and Mesoporous Materials*, **278**, 138–148.

28. Akpomie, K., Efeturi, O., Alumona, T. N. & Alum, O. L. (2017) Attenuation of Methylene Blue From Aqua media on Acid Activated Montmorillonite of Nigerian Origin. *Journal of Environmental Science and Management*, **20(2)**, 17–27.

29. Chen, Y., Zhu, B., Wu, D., Wang, Q., Yang, Y., Ye, W. & Guo, J. (2012) Eu(III) adsorption using di(2-thylhexly) phosphoric acid-immobilized magnetic GMZ bentonite. *Chemical Engineering Journal*, **181–182**, 387–396.

30. Yi, F. Y., Zhu, W., Dang, S., Li, J. P., Wu, D., Li, Y. H. & Sun, Z. M. (2015) Polyoxometalates-based heterometallic organic-inorganic hybrid materials for rapid adsorption and selective separation of methylene blue from aqueous solutions. *Chemical Communications*, **51(16)**, 3336–3339.

31. Zhang, Y., Zhu, C., Liu, F., Yuan, Y., Wu, H. & Li, A. (2019) Effects of ionic strength on removal of toxic pollutants from aqueous media with multifarious adsorbents: A review. *Science of the Total Environment*, **646**, 265–279.

32. Kang, S., Zhao, Y., Wang, W., Zhang, T., Chen, T., Yi, H., Rao, F. & Song, S. (2018) Removal of methylene blue from water with montmorillonite nanosheets/chitosan hydrogels as adsorbent. *Applied Surface Science*, **448**, 203–211.